KOSZALIN UNIVERSITY OF TECHNOLOGY
POLITECHNIKA KOSZALIŃSKA

Monograph

RESEARCH AND MODELLING IN CIVIL ENGINEERING 2017

Edited by
Jacek Katzer and Krzysztof Cichocki

KOSZALIN 2017

MONOGRAPH NO 338
FACULTY OF CIVIL ENGINEERING,
ENVIRONMENTAL AND GEODETIC SCIENCES

ISSN 0239-7129
ISBN 978-83-7365-474-7

Editors
Jacek Katzer, Krzysztof Cichocki
Koszalin University of Technology, Poland

Reviewers
Jacek Gołaszewski – Silesian University of Technology, Poland
Izabela Major – Częstochowa University of Technology, Poland

Technical editor
Czesław Suchocki

Website editor
Mariusz Ruchwa

Linguistic consultations
Ewa Sokołowska-Katzer

Typesetting
Czesław Suchocki

Cover design
Tadeusz Walczak
(Photo by *Jacek Katzer*)

KOSZALIN UNIVERSITY OF TECHNOLOGY PUBLISHING HOUSE
75-620 Koszalin, Racławicka 15-17, Poland

Koszalin 2017, 1st edition, publisher's sheet 7,8, circulation 100 copies
Printing: INTRO-DRUK, Koszalin, Poland

Table of contents

2. Dynamic numerical analysis of the integrated shear connection

Maciej Major[1], Paweł Helbrych[2]
[1,2] *Politechnika Częstochowska, Wydział Budownictwa, Częstochowa, Polska*

2.1. Introduction

Development of integrated structures is closely correlated with the development of technologies to obtain framing structures, where integrated components are often preferred. The most frequently used and the most effective solution is integrated floor structures, with reinforced concrete slab on the fluted sheet metal is integrated with the girder made of a steel section (in typical solutions, the function of the girder is overtaken by the I beam) (Biliński, Kmita, 2009). It is necessary for the design of the integrated floors to take into consideration two stages: construction and use (Moy, Jolly, El Shihya, 1987). In the first phase, during calculation of the ultimate limit states and serviceability limit states, the functional load, weight of components and weight of concrete mixture should be also analysed. In this phase, the fluted sheet metal performs the role of the permanent formwork. In the second phase, the interrelations between the girder and the concrete slab should be evaluated, with loads compared in this phase being functional load and technological load, individual weights of structural components and finish layers. In the phase of use, the fluted sheet metal performs the role of the external reinforcement of the span reinforcement of the floor slab. In the case of typical integrated floors, the best integration of the slab with the steel section is ensured by the use of the non-welded connectors assembled mechanically, which ensures a substantial reduction of the assembly time for the whole construction component (Major, Major, 2015). The most frequently used non-welded connector is continuous connector in the form of a stripe of the fluted sheet metal with specific width or a shear connector Hilti X-HVB, both assembled by means of the nails shot with the nail gun (Thomas, O`Leary 1998).

In a study by (Nawrot, Kucharczuk, 2004), the authors presented an alternative solution in the form of the hat connectors, which their utility confirmed by the experimental examinations.

The aim of this chapter was to determine the compatibility of the numerical and experimental model by comparing the vertical displacement (slip) as a function of the applied load and the dynamic analysis of the discussed connection in which the hat-shaped connector was adopted.

2.2. Experimental tests

The PN-EN 1994-1-1 standard presents a model for examinations of connectors for integrated steel and concrete beams. According to the guidelines, the model is composed of two concrete slabs connected with the examined connectors using the steel section (I-beam). Fig. 2.1. The adequately prepared model is situated on the test stand and loaded with the axial force applied to the transverse upper surfaces of the I-beam, thus forcing the shear force in the integration plane. For individual increments of the axial force, the measurements of vertical displacements occurring in the plane of contact of the concrete slabs with the steel section are made. The measured slips are used to evaluate the capacity and ductility of the connector. According to the PN-EN 1994-1-1 standard, the ductile connectors are those with sufficient deformation capacity to justify the assumption of ideal plastic behaviour of the shear connection in the structure considered, whereas those that do not meet this assumption are considered as non-ductile.

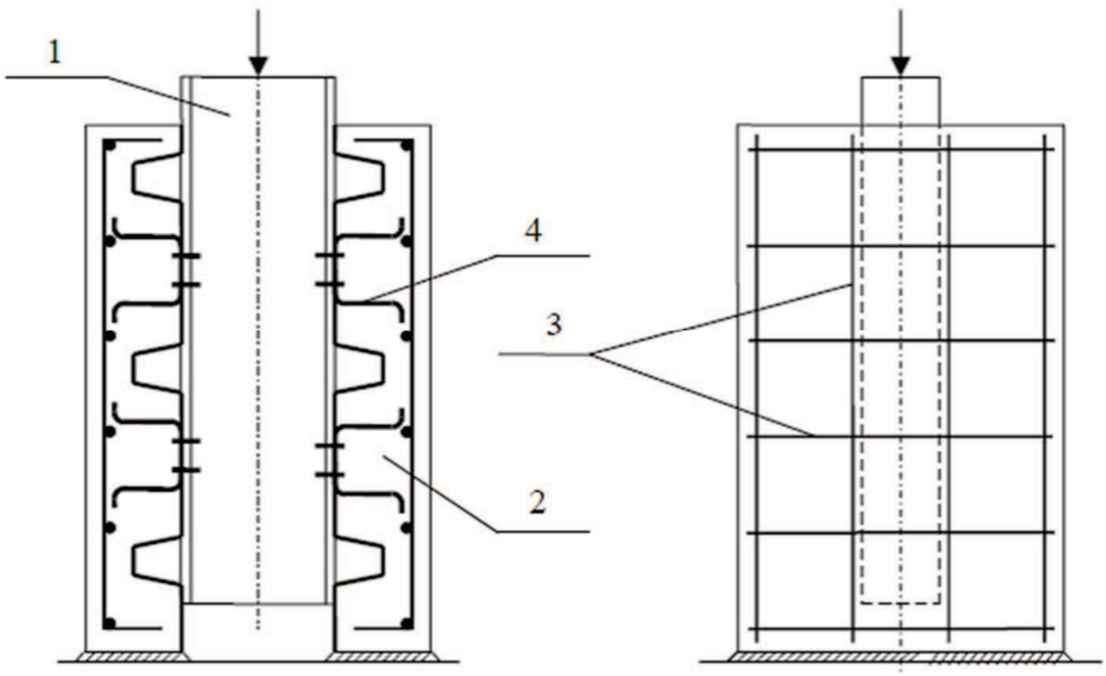

Fig. 2.1. Model of shear connector: 1- steel section, 2 - concrete slab on fluted sheet, 3 – slab reinforcement, 4 - connector tested (photo Nawrot, Kucharczuk, 2004)

The experimental tests were performed for three models with 100 mm connectors and three similar models with 60 mm connector. Figure 2.2 presents a geometry of the connector.

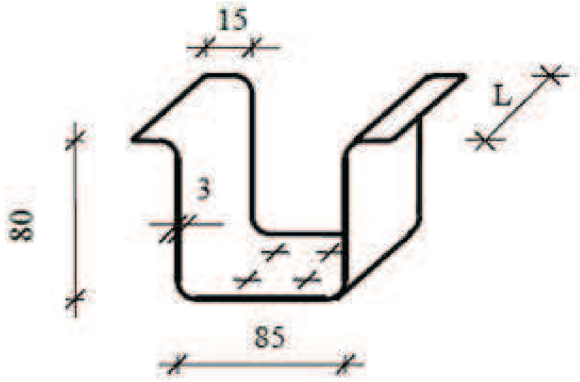

Fig. 2.2. Hat-shaped connector (photo Nawrot, Kucharczuk, 2004)

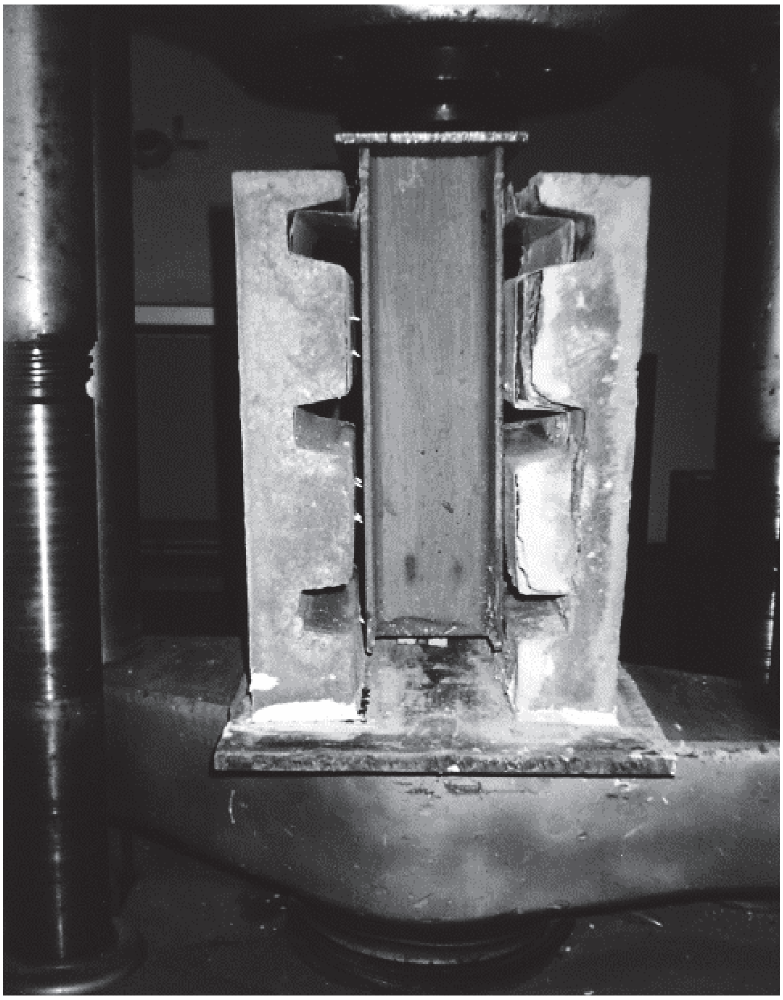

Fig. 2.3. Form of the destruction of the examined shear connection (photo Nawrot, Kucharczuk, 2004)

The models were prepared for the following geometrical and material data:

a) steel section:

- type: HEA 160,
- steel S235.

b) concreted slab:

- dimensions: 105x400x550 mm,
- concrete C25/30,
- reinforcement Ø 10, steel AII,
- trapezoidal metal sheet T55x188, thickness 0.75 mm.

c) hat-shaped connector:

- geometry according (Fig. 2.2),
- steel S235,
- 4 x nail Ø 4.5 ENP Hilti.

During the experiment, the capacity of the connectors and slips in the model were evaluated and the forms of destruction of the connection were analysed (see Fig. 2.3).

2.3. Numerical model of the connection

Numerical calculations were performed using the ANSYS software based on the finite element method. All the elements of the shear model were made as 10-node Solid elements. The model was loaded with its own weight and the force distributed on the upper surface of the I-beam HEA160. The support was modelled as a movable support (Fig. 2.4).

An elastic-plastic model was adopted for the HEA160 section, with the following parameters:

- density: 7.850 kg/m^3,
- Poison's ratio: 0.3,
- Young's modulus: 210 GPa,
- yield point: 292.25 MPa (determined empirically),
- ultimate tensile strength: 405.15 MPa (determined empirically).

An elastic-plastic model of material was adopted for the 60 mm hat-shaped connector, with the following parameters:

- density: 7850 kg/m^3,
- Poison's ratio: 0.3,
- Young's modulus: 210 GPa,
- yield point 332.20 MPa (determined empirically),
- ultimate tensile strength: 415.25 MPa (determined empirically).

A elastic-plastic model of material was adopted for the trapezoidal sheet metal, with the following parameters:

- density: 7850 kg/m^3,
- Poison's ratio: 0.3,
- Young's modulus: 210 GPa,
- yield point 277.25 MPa (determined empirically),
- ultimate tensile strength: 350.10 MPa (determined empirically).

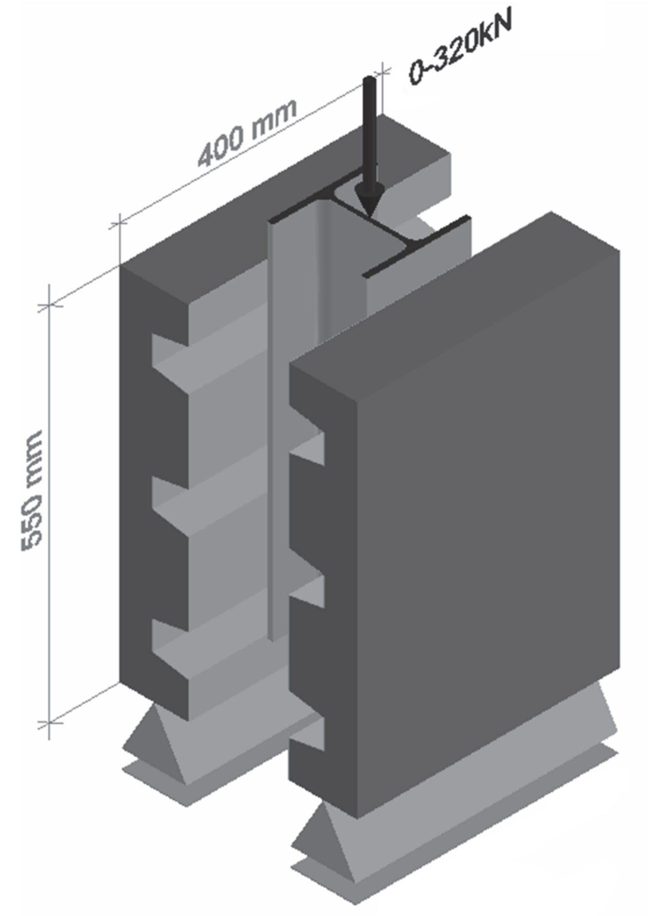

Fig. 2.4. The numerical model of the shear connection

A model of material was adopted for the concrete, with the following parameters:

- density: 2500 kg/m^3,
- Poison's ratio: 0.2,
- Young's modulus: 30 GPa,
- compression strength: 16.08 MPa.

An elastic-plastic model of material was adopted for the nails, with the following parameters:

- density: 7850 kg/m^3,
- Poison's ratio: 0.3,

- Young's modulus: 200 GPa,
- yield point 350.0 MPa,
- ultimate tensile strength: 650.0 MPa.

An elastic-plastic model of material was adopted for the reinforcement bars, with the following parameters:

- density: 7850 kg/m^3,
- Poison's ratio: 0.3,
- Young's modulus: 205 GPa,
- yield point 305.0 MPa,
- ultimate tensile strength 490 MPa.

The Tetrahedrons method was used to generate a model grid, using quadrilateral 10-node elements (see Fig. 2.5).

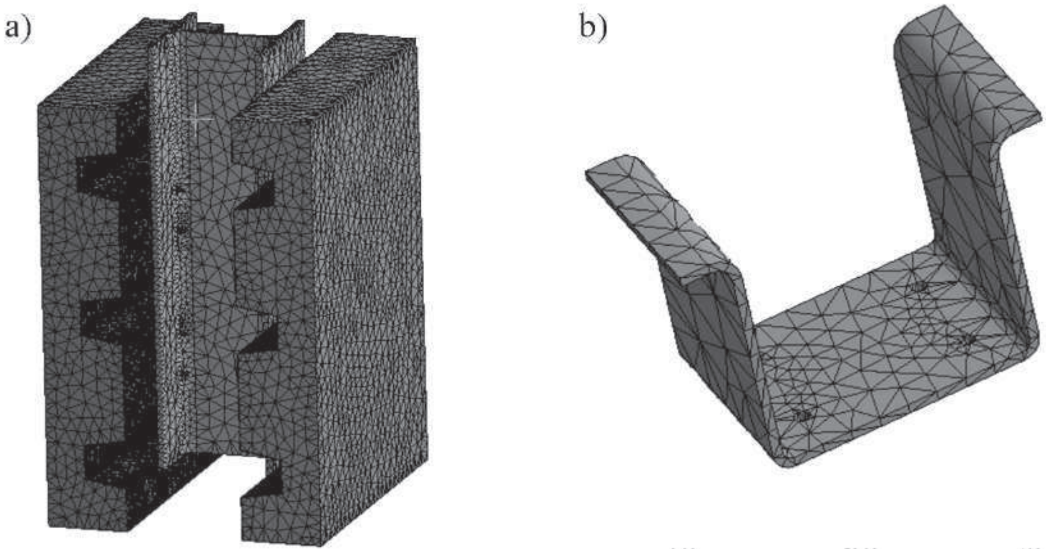

Fig. 2.5. Element grid: a) examined model, b) hat-shaped connector

2.4. Static examination of the numerical model

The model No. 6 with 60 mm hat-shaped connector, examined empirically in a study by [Nawrot, Kucharczuk, 2004] was adopted as a reference model for the numerical static examination. In order to verify the consistency of the experimental and numerical models, the comparison was made for the displacement as a function of the applied load for both models.

The experimental model and numerical models were loaded with the axial load in the range of from 0 kN to 330 kN, with the steps of 15, 10 and 5 kN. The load for the numerical model was completed for the value of the destructive force of the empirical model. The vertical displacement at the moment of the experimental model destruction was 3.50 mm and the slab was disconnected at the locations of the connectors.

Figure 2.6 presents the values of loading forces and slips for the experimental and numerical models.

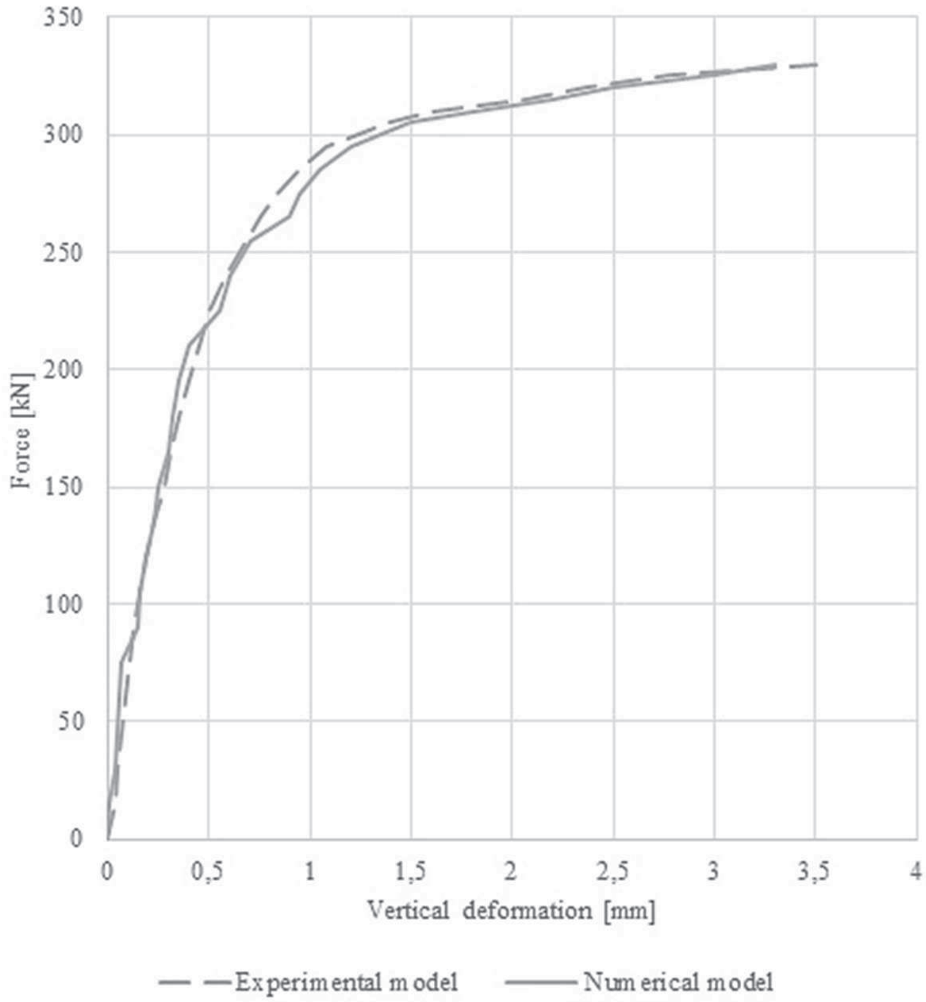

Fig. 2.6. The slip between the concrete slab and the HEA160 steel section: a) experimental model b) numerical model

For the numerical model, the highest vertical deformation (slip in the plane of contact of the HEA160 I-beam with the concrete slab) was established for the maximal shear force of 330 kN and was 3.38 mm. The slips obtained for individual values of loading forces in the numerical model can be regarded as consistent with the results of the experiments, which suggest the adequate modelling of the shear connector in the numerical analysis.

The greatest overall deformation in the numerical model was observed for the sheet metal at the contact with the concrete slab for the maximal shear force of 330 kN. Furthermore, the trapezoidal sheet metal was disconnected from the concrete slab as shown in Fig. 2.7, whereas Fig. 2.8 illustrates overall deformations in the experimental model.

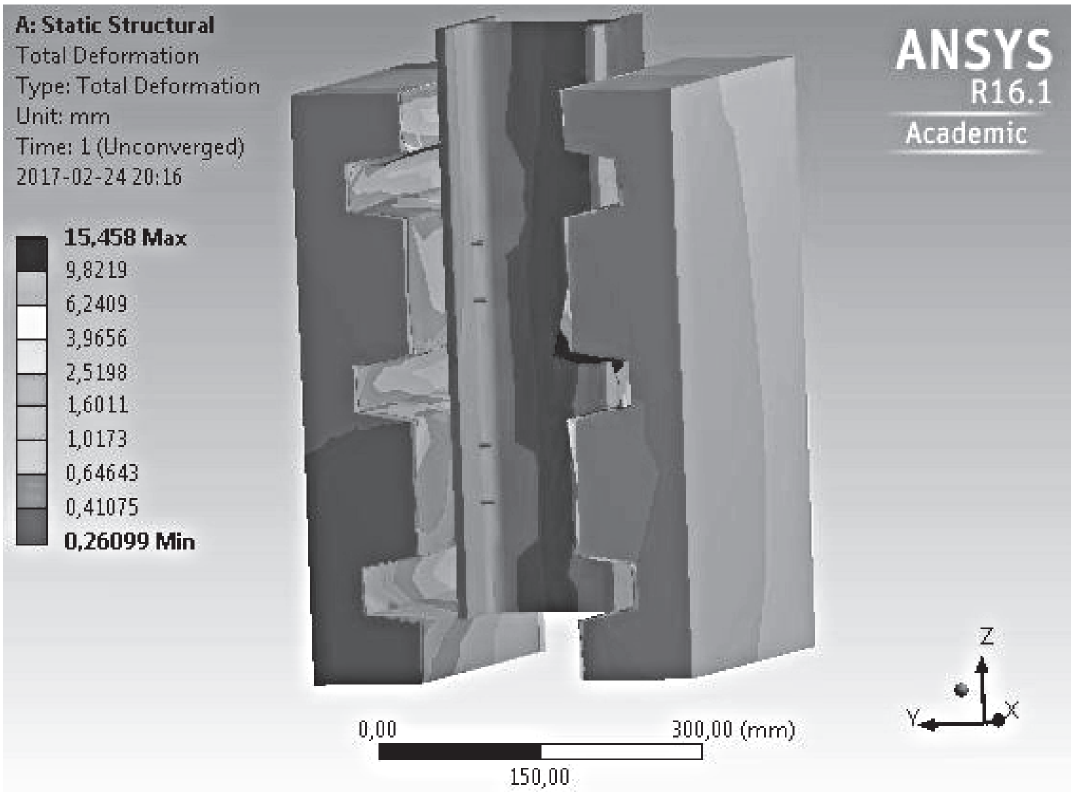

Fig. 2.7. General deformations of the analysed numerical model of the shear connection

In the numerical model, the locations of concentration of shear stresses are near the lower wall of the hat-shaped connectors in the area of integration of the I-beam with the concrete slab, see Fig. 2.9a

Furthermore, the maximal shear stresses (381.54 MPa, see Fig. 2.9b) in the hat-shaped integration connector were observed in the location of the contact between the horizontal and vertical walls of the connector. Tensile strength of the connector was not exceeded, whereas this was the case for the yield point, which is consistent with the experimental tests, where the connector was plastically deformed, but the material was not broken.

Fig. 2.8. General deformations of the analysed experimental model of the shear connection (photo Nawrot, Kucharczuk, 2004)

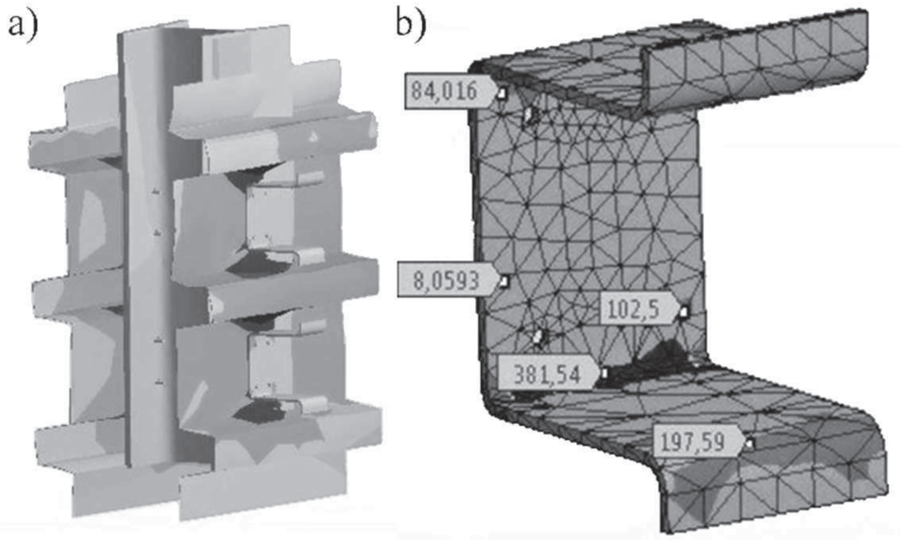

Fig. 2.9. Shear stresses in the numerical model: a) locations of stresses concentration, b) shear stresses in the connector

2.5. Dynamic examination of the numerical model

After the initial numerical analysis of the shear model of the integrated connection and obtaining the consistency of the results of the slips of the steel I-beam (HEA160) with the experimental and numerical analyses, the dynamic analysis of the model of the shear connection was conducted. The numerical model was loaded for 9 times with the axial force, with initial value of the axial force of 50 kN, incremented with five steps of 300 kN and the sixth step of 20 kN to the level of 320 kN. Next two steps were reducing the loading force to the values of 300kN and 200kN, respectively. Total time of the application of the axial force was 9.1×10^{-5} s, whereas total time of load analysis was 4×10^{-4} s. The range of values of load with the axial forces is identical in its value to the static load in the experimental examinations for the model No. 5, whereas time of its effect was selected for the speed of sound wave propagation in the solid body under normal conditions of 5.100 m/s. The design of the load to the numerical model is presented in Fig. 2.10.

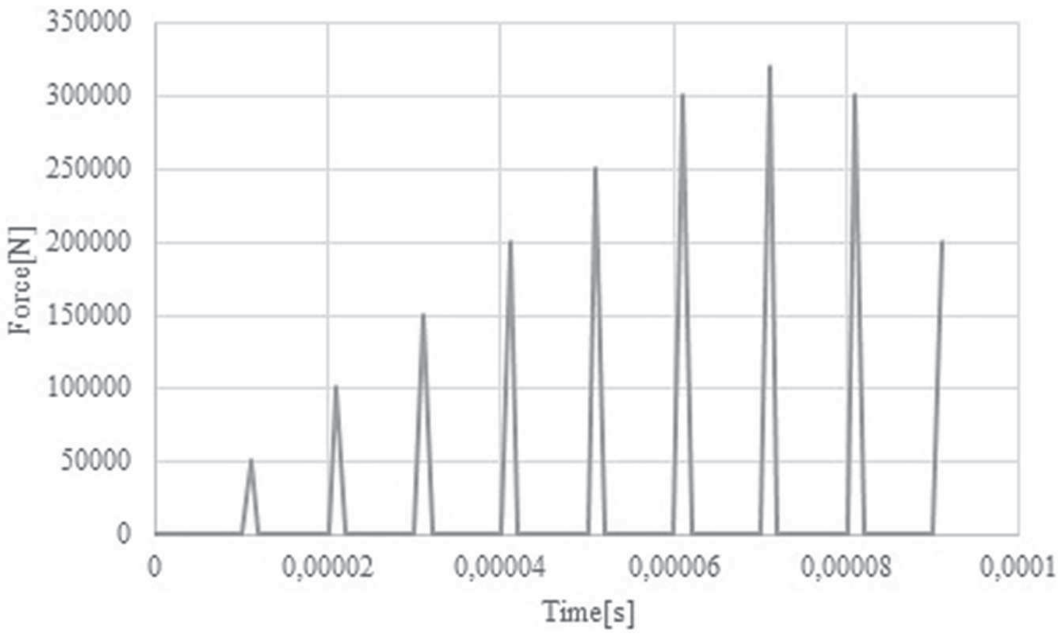

Fig. 2.10. Design of the load to the numerical model

In the loading phase, i.e. in the period from 0 to 9.1×10^{-5} the layered distribution of stresses was observed, with no maximal stresses obtained for the time of analysis. Maximal stresses in this period were 109.3 MPa. It is also noticeable that stresses are transferred through the connectors to the concrete slabs (Fig. 2.11).

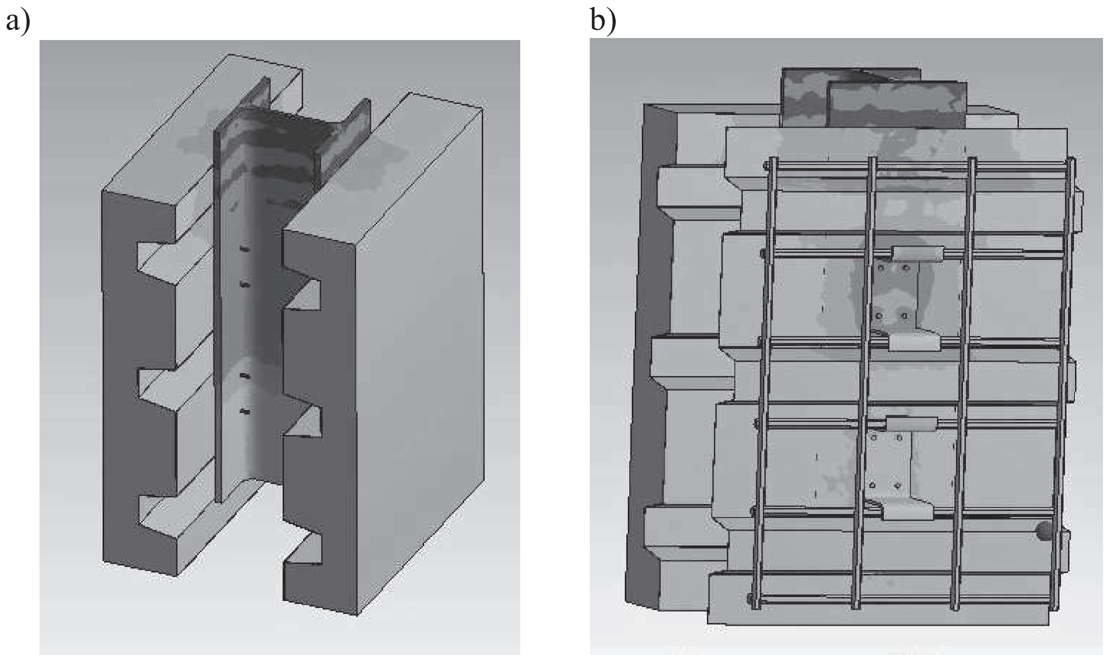

Fig. 2.11. Distribution of stresses in the model studied in the loading phase: a) view of the whole model, b) view without concrete slab

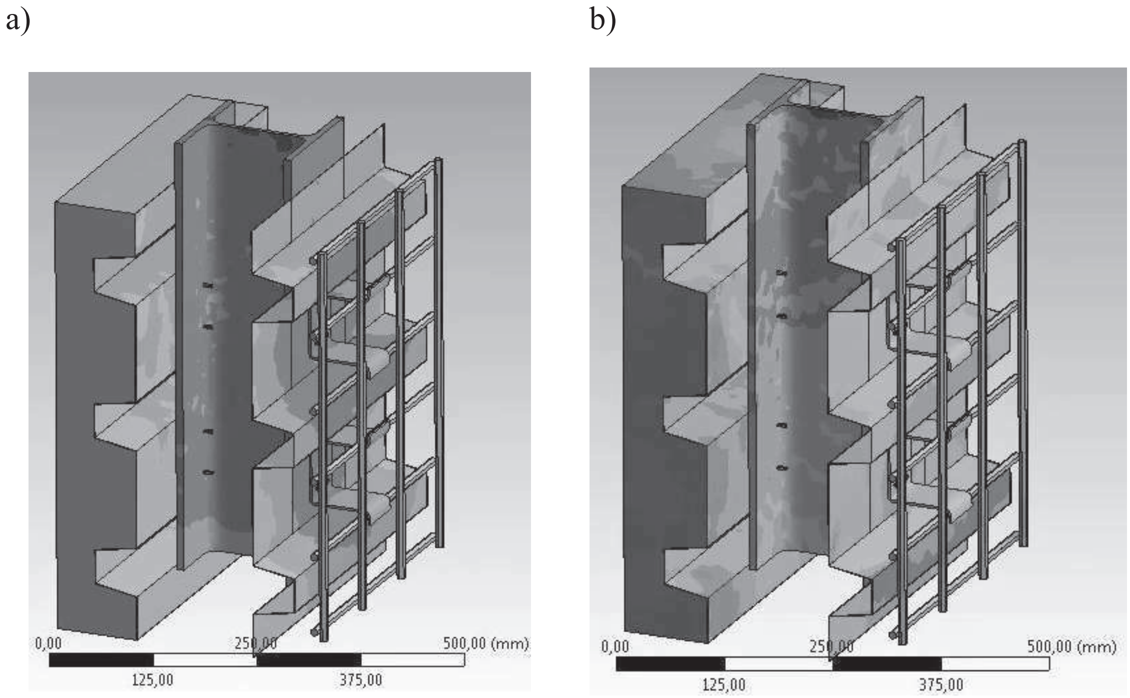

Fig. 2.12. Distribution of stresses in the model in the phase of analysis: a) distribution of stresses for 1.6×10^{-4} s, b) distribution of stresses for 3.2×10^{-4} s

In the initial phase of the analysis, i.e. from 9.1×10^{-5} s to 2×10^{-4} s, a uniform distribution of stresses was observed in the whole model and the spectrum of load effect was extended in the concrete slab (see Fig. 2.12a); for the analysis time of 1.6×10^{-4} s, the maximal shear stresses were 201.77 MPa.

In the final phase of the analysis, i.e. from 2×10^{-4} s to 4×10^{-4} s, scattering of the wave of shear stress and gradual reduction of the stress value in the function of time were observed in the model (see Fig. 2.12b).

Analysis of the distribution of shear stresses in the connector revealed their concentration near the holes for nails, with maximal values of stresses observed at the same time for the whole model i.e. 1.6×10^{-4} s, reaching 63.8 MPa (Fig. 2.13).

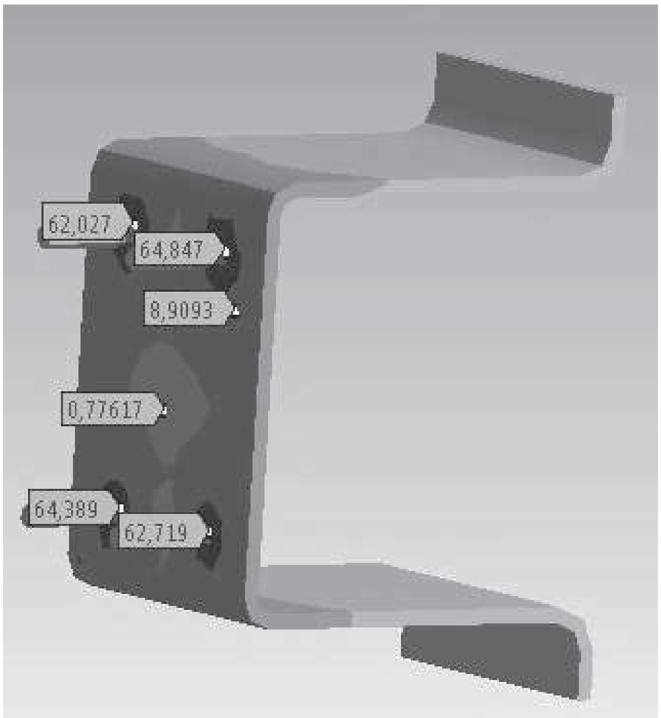

Fig. 2.13. Distribution of shear stresses in the hat-shaped connector

Values of maximal shear stresses vs time are presented in Fig. 2.14.

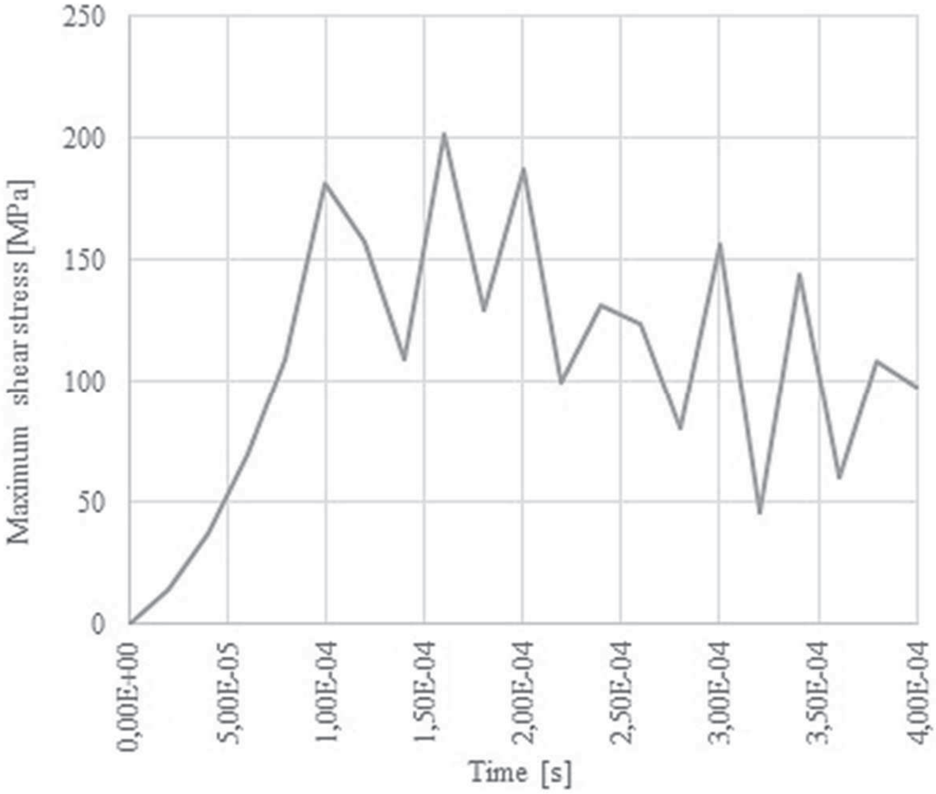

Fig. 2.14. Design of the load to the numerical model

2.6. Conclusions

The numerical model correctly maps the behavior of a shear connection made using a hat-shaped connector. The shear stresses for the numerical model were consistent with the results obtained in the experimental studies. A high convergence of slip curves for both methods was obtained, with a maximum difference of 4.4%. Shear stresses in all model elements did not exceed the limit values either for the experimental or numerical analyses. Yield of the hat-shaped connector was not observed in the dynamic analysis. The proposed numerical model can be used to pre-verify different variants of the connector geometry to optimize its shape.

References

Biliński T., Kmita J., *Dorobek nauki polskiej w zakresie konstrukcji zespolonych.* Zielona Góra: Oficyna Wydawnicza Uniwersytetu Zielonogórskiego, 2009.

Bródka J., Kozłowski A., *Stalowe budynki szkieletowe*. Rzeszów: Oficyna Wydawnicza Politechniki Rzeszowskiej. 2003.

Major M., Major I. *Konstrukcje zespolone w budownictwie zrównoważonym*, Budownictwo o zoptymalizowanym potencjale energetycznym, nr (16), Częstochowa 2015, pp. 51-56.

Moy S., Jolly C., El Shihya A., *Unwelded Shear Connectors for Composite Beams*, Composite Steel Structures, London-New York, 1987, pp. 65-74.

Nawrot J., Kucharczuk W., *Badanie nośności nowych łączników do zespolonych stropów stalowo-betonowych*, Inżynieria i Budownictwo, 2004, R.60 nr 12, pp. 654-657.

PN-EN 1994-1-1 Eurokod 4 2008, .*Projektowanie zespolonych konstrukcji stalowo-betonowych*, Część 1-1: Reguły ogólne i reguły dla budynków, Bruksela.

Thomas D., O`Leary D.C., *Composite beams with profiled-steel sheeting and non welded shear connectors*, Steel Construction To-day, 1998, Vol. 2 No. 4, pp. 117-121.